J. of Supercritical Fluids 88 (2014) 66–73

Contents lists available at ScienceDirect

The Journal of Supercritical Fluids

journal homepage: www.elsevier.com/locate/supflu

# Polycarbonate foams with tailor-made cellular structures by controlling the dissolution temperature in a two-step supercritical carbon dioxide foaming process

Gabriel Gedler, Marcelo Antunes, José Ignacio Velasco *

*Centre Català del Plàstic, Departament de Ciència dels Materials i Enginyeria Metal·lúrgica, Universitat Politècnica de Catalunya BarcelonaTech (UPC), C/Colom 114, E-08222 Terrassa, Spain*

ARTICLE INFO

*Article history:*
Received 5 November 2013
Received in revised form 21 January 2014
Accepted 22 January 2014
Available online 7 February 2014

*Keywords:*
Polycarbonate foams
Supercritical carbon dioxide
Two-step foaming
Tailor-made cellular structure
Physical aging

ABSTRACT

Closed-cell polycarbonate foams were prepared using a two-step foaming process, which consisted of the initial dissolution of supercritical $CO_2$ ($scCO_2$) into PC foaming precursors and their later expansion by heating using a double contact restriction method. The effects of the parameters of both $CO_2$ dissolution and heating stages on the cellular structure characteristics as well as on the physical aging of PC in the obtained foams were investigated. A higher amount of $CO_2$ was dissolved in PC with increasing the dissolution temperature from 80 to 100 °C, with similar $CO_2$ desorption trends and diffusion coefficients being found for both conditions. PC foams displayed an isotropic-like microcellular structure at a dissolution temperature of 80 °C. It was shown that it is possible to reduce their density while keeping their microcellular structure with increasing the heating time. On contrary, when dissolving $CO_2$ at 100 °C and later expanding, PC foams presented a cellular morphology with bigger cells and with an increasingly higher cell elongation in the vertical growth direction with increasing the heating time. Comparatively, PC foams obtained by dissolving $CO_2$ at 100 °C presented a more marked physical aging after $CO_2$ dissolution and foaming, although this effect could be reduced and ultimately suppressed with increasing the heating time.



## 1. Introduction

The use of supercritical carbon dioxide ($scCO_2$) has become one of the most common strategies to prepare thermoplastic-based polymer foams. The processing conditions used in both gas dissolution and expansion stages play an essential role in the characteristics of the resulting foams, as for instance it is known that carbon dioxide acts as polymer plasticizer, decreasing its glass transition temperature [1]. As a result, the expansion is facilitated due to decreased polymer viscosity, easily leading to cell coalescence and as a consequence to an increase in cell size and a decrease in cell density [2].

The dissolution of $scCO_2$ into polymers and later expansion is commonly done in one [3] or two stages [4], in this last case the first stage corresponding to $CO_2$ dissolution into the polymer and the second one to its expansion. Particularly, polycarbonate (PC) foams have been prepared inside high pressure vessels using $scCO_2$ and one-step or two-step expansion [5,6]. In the case of two-step foaming, the expansion stage is done either inside the same vessel used to initially dissolve the carbon dioxide or in oil baths in order to foam the gas-saturated samples obtained at the end of the dissolution stage [7–9]. Two-step foaming has been shown to present the advantage of effectively separating cell nucleation from cell growth, ultimately leading to the formation of foams with a wide range of foam densities and a microcellular core structure with cell nucleation densities in the order of $10^9$ cells/cm$^3$. Likewise, $CO_2$ dissolution during the first step enables to reduce the temperature required to nucleate and grow the cells, as $CO_2$ has a plasticizing effect on the polymer, significantly reducing its glass transition temperature, thus enabling for a better control of the developed cellular morphology (smaller and more isotropic-like cells) and, as a result, of the physical properties of the foamed materials [9].

In amorphous polymers such as PC cooled below their glass transition temperature, as happens during $CO_2$ dissolution in a foaming process, the molecules can be frozen-in at a non-equilibrium state, with later annealing resulting in an enthalpy relaxation towards an equilibrium state, resulting in changes in the structure and as a consequence in the physical properties of the polymer [10]. This enthalpy relaxation, known as physical aging [10], can be detected by the appearance of an endothermic peak in the glass transition of the polymer using experimental techniques such as

* Corresponding author. Tel.: +34 937837022; fax: +34 937841827.
*E-mail addresses:* gabriel.gedler@upc.edu (G. Gedler), marcelo.antunes@upc.edu (M. Antunes), jose.ignacio.velasco@upc.edu (J.I. Velasco).

0896-8446/$ – see front matter © 2014 Elsevier B.V. All rights reserved.
http://dx.doi.org/10.1016/j.supflu.2014.01.013

differential scanning calorimetry (DSC) [11,12]. It has been shown that mechanical properties of PC such as the elastic modulus and hardness increase with aging while others such as the impact strength decrease [13], which has been related to an increasingly higher free volume relaxation of the polymer, although no simple correlation has been established between these mechanical properties and changes in the endothermic glass transition peak resulting from aging.

In this work we present the preparation using a two-step foaming process of closed-cell PC foams with tailored cellular structures that varied from isotropic-like microcellular to highly oriented and with bigger cells by controlling the dissolution temperature of $scCO_2$, as well as the effects of foaming on the physical aging of PC, as the cellular structure morphological aspects and relaxation state of PC are of extreme importance in terms of regulating the final properties of the resulting foams.

## 2. Materials and methods

### 2.1. Preparation of PC foam precursors

Polycarbonate (Lexan-123R-PC, supplied by Sabic in the form of pellets), with a density of 1.2 g/cm$^3$ and melt flow index (MFI) of 17.5 dg/min, measured at 300 °C and 1.2 kg, was compression-moulded at 220 °C and 45 bar in a hot-plate press (IQAP LAP PL-15) to circular-shaped plates with a thickness of 3.5 mm and diameter of 74 mm in three steps: (1) in the first step the PC pellets initially placed in the circular-cavity mould were softened at 220 °C during 10 min; (2) the second step consisted in removing possible air trapped between the PC pellets by initially pressurizing and releasing the pressure several times gradually increasing the pressure from 5 to 45 bar and keeping a constant pressure of 45 bar during 1 min at 220 °C; (3) in the third and last step the circular-cavity mould containing the PC was quickly transferred to the cooling station of the press, where it was cooled down for 5 min under a constant pressure of 45 bar. The circular-shaped PC plates obtained at the end of this step were used as foaming precursors. The samples used in the $CO_2$ desorption experiments were directly machined from these plates to a typical diameter value of 40 mm.

### 2.2. Foaming process: Stage I—Supercritical carbon dioxide dissolution

Once obtained by compression-moulding, the PC foam precursors were foamed by placing them inside a high pressure vessel and initially dissolving supercritical carbon dioxide ($scCO_2$). Two $scCO_2$ dissolution temperatures were used: 80 and 100 °C, in both cases applying a total dissolution time of 210 min. The $scCO_2$ was introduced in the vessel at room temperature at a pressure of 70 bar, reaching a final dissolution pressure of 140 and 170 bar, respectively, for a dissolution temperature of 80 and 100 °C. Once carbon dioxide was dissolved into the foam precursors, these were cooled down to room temperature by re-circulating water through the vessel's cooling jacket while keeping the vessel pressurized at 15 °C/h. After slow depressurization of the $scCO_2$ at room temperature, the PC foam precursors containing $CO_2$ were taken out from the vessel and left to stabilize at room temperature and atmospheric pressure for 120 min. Analysis of the internal morphology of the PC foam precursors containing $CO_2$ did not show any pre-foaming.

### 2.3. Foaming process: Stage II—Double contact restricted foaming

The PC foam precursors containing $CO_2$ obtained at the end of Stage I were once again placed in the circular-cavity mould and foamed in the hot-plate press by compression-moulding at a constant temperature of 165 °C and constant pressure of 60 bar. The circular-cavity mould and metal plates used in this stage were pre-heated at 165 °C prior to positioning of the precursors and foaming. The compression-moulding double contact used in this stage guaranteed the homogeneous heating of the precursors and ensured flatness of the surfaces for later characterization. After applying a heating time that varied between 40 and 120 s, the applied pressure was suddenly released, allowing the PC foam precursors containing $CO_2$ to expand in both vertical and width directions. After the expansion, the obtained foams were quickly removed from the plates and left to cool at room temperature by direct contact with air.

### 2.4. $CO_2$ desorption experiments

Desorption experiments were carried out in order to measure the $CO_2$ diffusion coefficient in PC for the two different dissolution temperatures. As previously mentioned, the samples used in these experiments were directly obtained from the PC foam precursors by reducing their diameter to 40 mm. After applying the conditions already indicated in Stage I of the foaming process, i.e., a $scCO_2$ dissolution temperature of 80 or 100 °C and pressure of 140 or 170 bar for a total dissolution time of 210 min, samples were cooled down to room temperature, removed from the vessel and quickly transferred to a balance in order to record the evolution of $CO_2$ mass loss with the desorption time.

The maximum concentration of $CO_2$ in the samples after decompression ($M_0$) was calculated by extrapolating to zero desorption time following the initial slope method [14]. Assuming one-dimensional diffusion in a plane sheet, the $CO_2$ diffusion coefficient ($D_d$) was determined by plotting $M_t/M_0$ as a function of $t/l^2$, where $M_t$ is the $CO_2$ concentration at time $t$ and $l$ is the thickness of the sample, according to the following equation [15]:

$$\frac{M_t}{M_0} = 1 - \frac{8}{\pi^2}\exp\left(-\frac{D_d t}{l^2}\right) \quad (1)$$

The $CO_2$ diffusion coefficient was determined from the slope of the $M_t/M_0$ vs. $t/l^2$ curve taking into account the last data range and the calculated value of $M_0$.

### 2.5. Cellular structure characterization

The density of the several PC foams was measured according to standard procedures (ISO 845), while the relative density was calculated by dividing this value by the density of the unfoamed precursor. Scanning electron microscopy (SEM) was used to analyze the cellular structure of the foams. Samples were prepared by cryogenically fracturing the foams in liquid nitrogen and sputter depositing a thin layer of gold at their surface using a BAL-TEC SCD005 Sputter Coater (argon atmosphere). Micrographs were obtained using a JEOL JSM-5610 scanning electron microscope applying a voltage of 10 kV and a working distance of 40 mm.

The average cell sizes in the vertical ($\phi_{VD}$) and width ($\phi_{WD}$) foaming directions were measured using the intercept counting method [16]. The cell aspect ratio (AR) was determined by dividing the value of the average cell size in the vertical direction by that measured in the horizontal one, i.e., $AR = \phi_{VD}/\phi_{WD}$. The cell nucleation density ($N_f$, in number of cells per volume of unfoamed material) was calculated using the following equation:

$$N_f = \left(\frac{n}{A}\right)^{3/2}\left(\frac{\rho_s}{\rho_f}\right) \quad (2)$$

where $n$ is the number of cells per area $A$ of micrograph (in cm$^2$) and $\rho_s$ and $\rho_f$ are, respectively, the solid and foam densities.

### 2.6. Differential scanning calorimetry analysis

Analysis by DSC was carried out on the obtained PC foams using a Perkin Elmer, Pyris 1 DSC model with a glycol-based Perkin Elmer Intracooler IIP. Heating curves were recorded at a heating rate of 10 °C/min from 30 to 300 °C using samples with a typical weight of 5.0 mg. The glass transition temperature ($T_g$) of PC was measured using the inflection point heat capacity method. Furthermore, the enthalpy relaxation corresponding to the glass transition was analyzed and quantified by measuring the area below the associated endothermic signal [17]. The values presented in this work are the result of the average of three measurements done for each foaming condition.

## 3. Results and discussion

### 3.1. $CO_2$ desorption kinetics and diffusion coefficient

The dissolution of $scCO_2$ in PC resulted in a maximum concentration of dissolved $CO_2$ ($M_0$) of 61.8 and 68.5 mg of $CO_2$/g of PC, respectively, for a dissolution temperature of 80 and 100 °C. The higher concentration of $CO_2$ dissolved in PC at the higher temperature (7 wt% $CO_2$ at 100 °C, compared to the 5 wt% of $CO_2$ dissolved at 80 °C) was related to the higher molecular mobility of PC in said conditions. The $CO_2$ desorption curves displayed in Fig. 1(a) show the evolution of the $CO_2$ concentration with the square root of the desorption time for the two dissolution temperatures, which, assuming a desorption behaviour according to Eq. (1), resulted in a $CO_2$ diffusion coefficient ($D_d$) of $6.86 \times 10^{-12}$ and $3.50 \times 10^{-12}$ $m^2/s$, respectively, for 80 and 100 °C (see Fig. 1(b) and embedded curve fit equations). Although there were slight differences between the two dissolution temperatures in terms of the amount of $CO_2$ initially dissolved in the samples, not only the evolution trend was similar but also both of these results were comparable to those found in literature for PC, where $D_d$ was found to be within $2.55 \times 10^{-11}$ and $4.60 \times 10^{-12}$ $m^2/s$ [18] or between $1.55 \times 10^{-12}$ and $6.93 \times 10^{-12}$ $m^2/s$ [19].

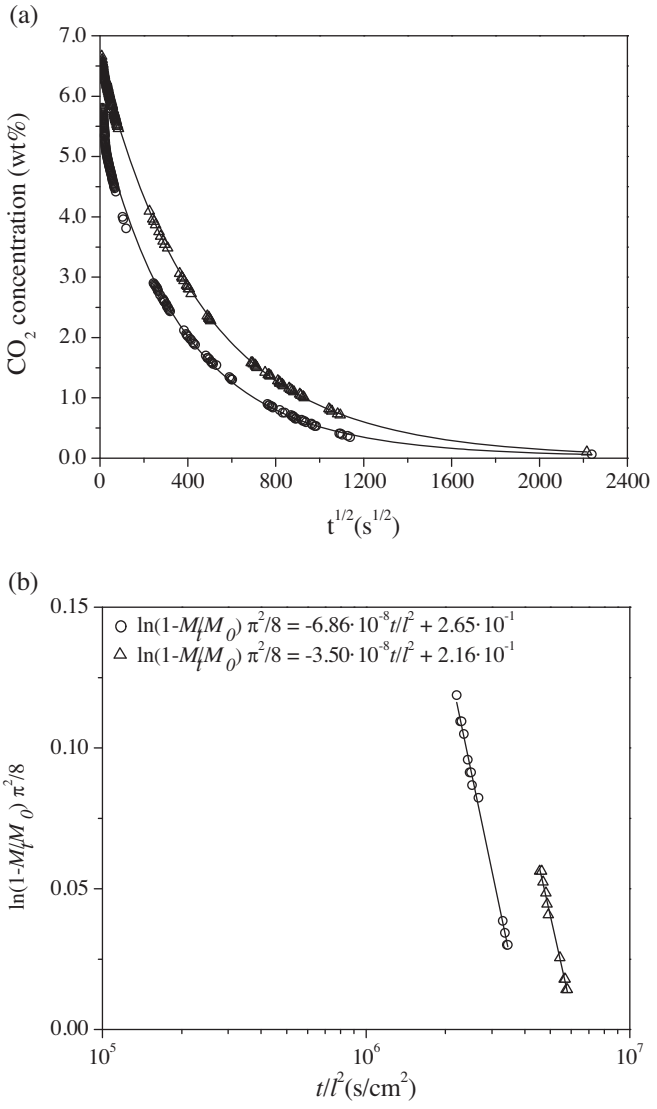


**Fig. 1.** (a) $CO_2$ desorption curves for PC with $CO_2$ dissolved at 80 °C (hollow circles) and 100 °C (hollow triangles) and (b) curve fits used to determine the $CO_2$ diffusion coefficient ($D_d$) according to Eq. (1).

### 3.2. Influence of the temperature of $CO_2$ dissolution on the cellular structure

As can be seen by the cellular structure characterization results presented in Tables 1 and 2, respectively, for a $CO_2$ dissolution temperature used in Stage I of foaming of 80 and 100 °C, depending on the $CO_2$ dissolution temperature it was possible to obtain closed-cell PC foams with relative densities between 0.15 and 0.07 and cellular structures that varied from globally isotropic-like microcellular (dissolution temperature: 80 °C) to cellular structures characterized by much bigger cells preferentially oriented in the vertical foam growth direction (dissolution temperature: 100 °C).

More specifically, the cellular structure morphology of all PC foams could be divided in two main zones, clearly differentiated in terms of cell size and cell orientation (see Fig. 2): an isotropic-like microcellular structure formed towards the centre of the sample (Zone I), which represented the main and dominant cellular morphology of the foams obtained by dissolving $CO_2$ at 80 °C, and a second zone (Zone II) with bigger cells elongated in the direction of pressure release (VD direction), which, in the case of the foams prepared by dissolving $CO_2$ at 80 °C was found near the upper and lower foam skins (see Fig. 2), while in the case of foams prepared by dissolving $CO_2$ at 100 °C it represented the main zone.

In the case of foams prepared by dissolving $CO_2$ at 80 °C, the first and dominant zone (Zone I), especially taking into account that the areas close to the surfaces are removed prior to further characterization, was formed as a result of a proper combination of $CO_2$ dissolution conditions (Stage I) and sudden pressure release after heating while restraining the expansion (Stage II). The formation of the second zone (Zone II) with much bigger cells was attributed to a non-uniform heat transfer at the end of Stage II, with the material remaining hotter at the surface due to direct contact with the metal plates used to restrict the expansion, which promoted cell coalescence.

As the main cellular morphology of PC foams prepared by dissolving $CO_2$ at 80 °C corresponded to Zone I, the cellular characterization analysis for these foams was carried out in this zone. Table 1 summarizes the main results of this analysis, indicating the average cell sizes in both VD and WD directions, cell nucleation density and cell aspect ratio, determined after analyzing several scanning electron micrographs at different magnifications. As can be seen, these foams presented a characteristic isotropic-like microcellular structure, with typical cell sizes that varied between 30 and 60 μm and cell nucleation densities $>10^8$ cells/$cm^3$.

While a temperature of $CO_2$ dissolution in Stage I of 80 °C ultimately resulted in PC foams with characteristic microcellular structures, PC foams obtained by dissolving $CO_2$ at 100 °C presented a cellular morphology with increasingly bigger and VD-elongated

**Table 1**
Cellular structure characterization results of PC foams prepared by dissolving $CO_2$ at 80 °C.

| Code | Heating time (s) | Relative density | $\phi_{VD}$ (μm) | $\phi_{WD}$ (μm) | $N_f$ (cells/cm$^3$) | AR |
|---|---|---|---|---|---|---|
| PC80-1 | 40 | 0.15 | 40 ± 3 | 40 ± 3 | $2.27 \times 10^8$ | 1.0 |
| PC80-2 | 60 | 0.14 | 34 ± 2 | 26 ± 2 | $3.72 \times 10^8$ | 1.3 |
| PC80-3 | 80 | 0.11 | 38 ± 3 | 37 ± 3 | $1.90 \times 10^8$ | 1.0 |
| PC80-4 | 100 | 0.08 | 58 ± 4 | 60 ± 4 | $4.96 \times 10^7$ | 1.0 |
| PC80-5 | 120 | 0.13 | 41 ± 3 | 47 ± 3 | $1.05 \times 10^8$ | 0.9 |

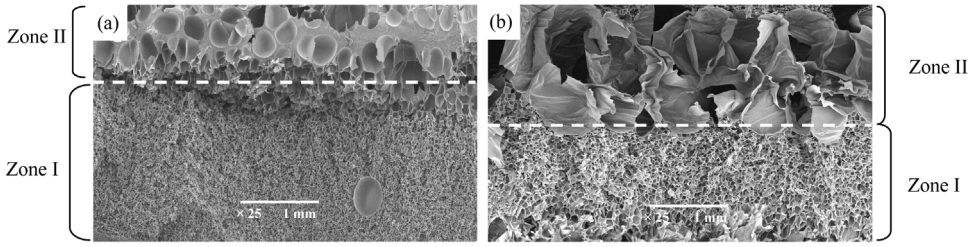


**Fig. 2.** Micrographs showing the typical cellular morphology of PC foams prepared by dissolving $CO_2$ at 80 °C: (a) 60 s and (b) 80 s of heating time applied during Stage II.

cells with increasing the heating time in Stage II, which, as can be seen by the micrographs displayed in Fig. 3 and the cellular structure characterization results presented in Table 2, resulted dominant after a heating time of 60 s. The cellular structure differences between PC foams obtained after dissolving $CO_2$ at 80 or 100 °C were attributed to the amount of $CO_2$ dissolved in the foam precursors during Stage I: 5 wt% $CO_2$ in the case of 80 °C and 7 wt% of $CO_2$ in the case of 100 °C.

### 3.3. *Influence of the heating time on the cellular structure*

As can be seen by the micrographs displayed in Fig. 4 for PC foams prepared by dissolving $CO_2$ at 80 °C and the ones shown in Fig. 3 for those obtained by dissolving $CO_2$ at 100 °C, the cellular morphology of PC foams was highly influenced by the heating time applied during Stage II.

A characteristic closed-cell structure was obtained for PC foams prepared by dissolving $CO_2$ at 80 °C, with average cell sizes between 30 and 60 μm depending on the heating time applied during Stage II. Direct result of the increase in heating time till 100 s, the relative density of PC foams decreased and as a result cells grew bigger (lower values of the cell nucleation density). The highest average cell sizes were observed for PC80-4 (around 60 μm), presenting values of the expansion ratio, defined as the quotient between the density of the foam and that of the solid material (i.e., the reciprocal of relative density), of 12. For a heating time of 120 s the cell size decreased as a consequence of the higher relative density of the resulting PC foam (PC80-5), which was attributed to a slight foam collapse after expansion, assessed by the fact that the cell aspect ratio resulted lower than 1 (i.e., $\phi_{WD} > \phi_{VD}$).

The characteristic cellular structure of PC foams prepared by dissolving $CO_2$ at 100 °C started to form at 60 s of heating time (see Fig. 3(b)). At these foaming conditions, PC foams (PC100-2) still presented two different cellular structure zones, with a zone with a microcellular structure (Zone I) similar to that of the foams obtained by dissolving $CO_2$ at 80 °C (cell sizes around 30 μm) but already with a dominant zone (Zone II) with bigger and elongated cells in the vertical foam growth direction (AR = 1.7). For heating times higher than 60 s PC foams prepared by dissolving $CO_2$ at 100 °C presented a cellular structure which was fully formed by these bigger and elongated cells (cell sizes around 600–700 μm and cell aspect ratios around 2.0). As with the foams obtained by dissolving $CO_2$ at 80 °C, PC foams where $CO_2$ was dissolved at 100 °C and that were heated in Stage II during longer times, more specifically for 120 s (PC100-5), presented higher relative densities and globally smaller cell sizes, once again attributed to a certain foam collapse after expansion (thus the slight decrease in *AR* for PC100-5 when compared to PC100-4).

The analysis of the influence of the foaming parameters on the cellular structure of PC foams allows establishing that, for a $CO_2$ dissolution temperature of 100 °C, there is a correlation with the heating foaming time applied in Stage II of both the relative density (see Fig. 5) as well as the cellular structure parameters of the foam (see Fig. 6 and the values presented in Table 2). On the contrary, at the lower $CO_2$ dissolution temperature of 80 °C it was possible to reduce the relative density of the resulting foam while keeping its microcellular structure.

As can be seen, not only it was possible to set the ideal heating time conditions in Stage II for obtaining PC foams with the minimum relative density, i.e., maximum expansion ratio (reaching expansion ratios up to 14), but also, depending on the temperature selected to dissolve $CO_2$ in Stage I, to prepare PC foams with very different cellular structures, from isotropic-like microcellular foams (cell sizes around 30–60 μm) to foams with a highly elongated cellular structure and much bigger cells (cell aspect ratios around 2.0).

In a similar way, Ma and co-workers recently reported on the fabrication using $scCO_2$ of microcellular PC foams with unimodal and bimodal cell-size distributions [20]. While one-step foaming was used to prepare unimodal PC foams above the

**Table 2**
Cellular structure characterization results of PC foams prepared by dissolving $CO_2$ at 100 °C.

| Code | Heating time (s) | Relative density | $\phi_{VD}$ (μm) | $\phi_{WD}$ (μm) | $N_f$ (cells/cm$^3$) | AR |
|---|---|---|---|---|---|---|
| PC100-1 | 40 | 0.15 | 25 ± 2 | 22 ± 2 | $8.02 \times 10^8$ | 1.1 |
| PC100-2 | 60 | 0.09 | 30 ± 2 | 26 ± 2 | $3.72 \times 10^8$ | 1.1 |
| | | | 488 ± 5 | 287 ± 5 | $2.27 \times 10^5$ | 1.7 |
| PC100-3 | 80 | 0.07 | 606 ± 6 | 358 ± 5 | $1.13 \times 10^5$ | 1.7 |
| PC100-4 | 100 | 0.07 | 710 ± 6 | 316 ± 5 | $1.11 \times 10^5$ | 2.2 |
| PC100-5 | 120 | 0.12 | 465 ± 5 | 237 ± 5 | $2.91 \times 10^5$ | 2.0 |

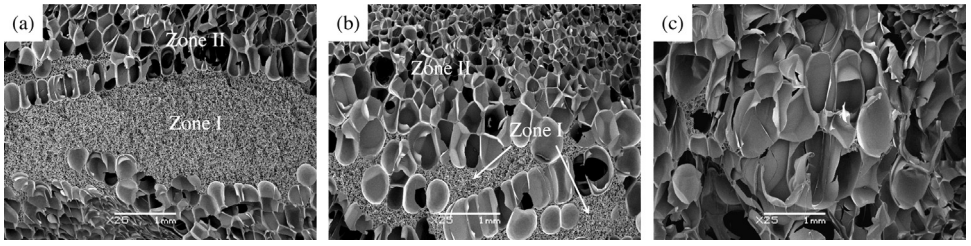


**Fig. 3.** Micrographs showing the typical cellular morphology of PC foams prepared by dissolving $CO_2$ at 100 °C: (a) 40 s, (b) 60 s and (c) 80 s of heating time applied during Stage II.

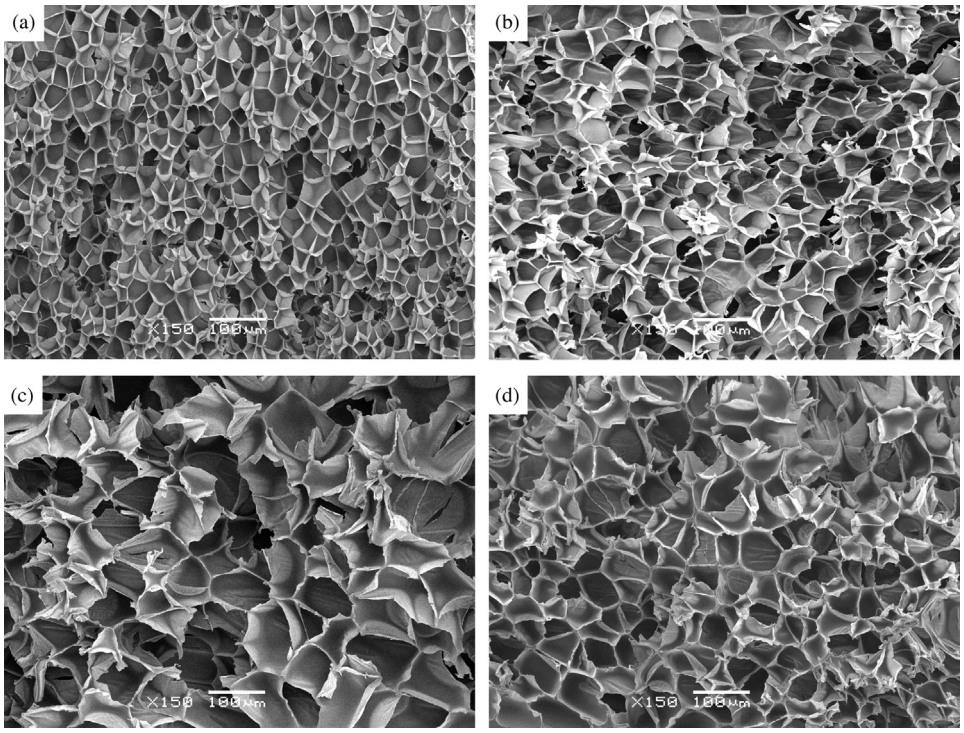


**Fig. 4.** Micrographs showing the characteristic microcellular morphology (Zone I) of PC foams prepared by dissolving $CO_2$ at 80 °C: (a) 60 s, (b) 80 s, (c) 100 s and (d) 120 s of heating time applied during Stage II.

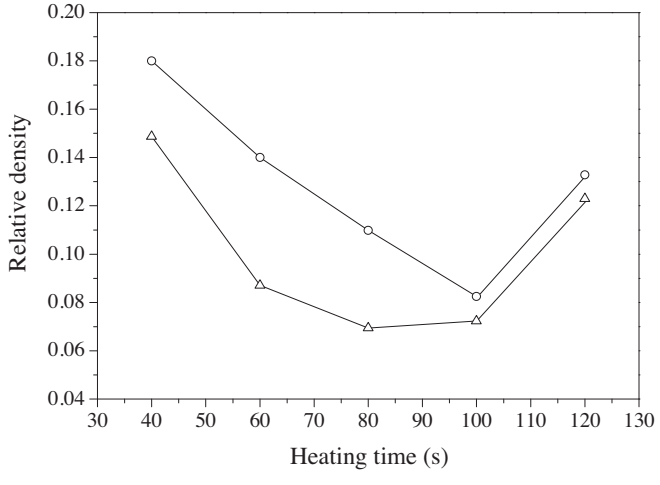


**Fig. 5.** Evolution of the relative density with the heating time applied during Stage II for PC foams prepared by dissolving $CO_2$ at 80 °C (hollow circles) and 100 °C (hollow triangles).

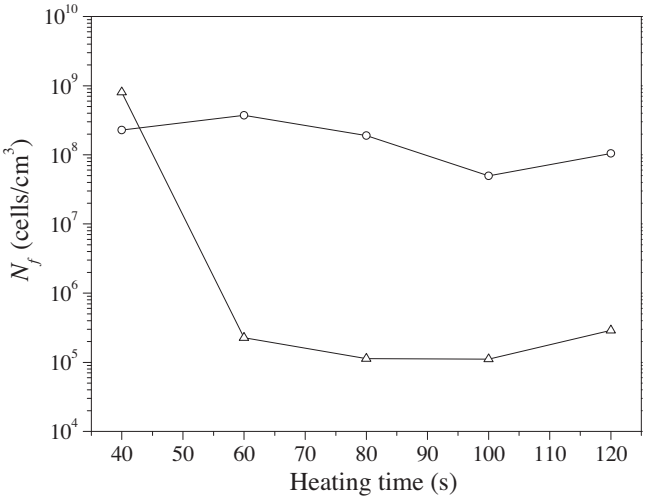


**Fig. 6.** Evolution of the cell nucleation density with the heating time applied during Stage II for PC foams prepared by dissolving $CO_2$ at 80 °C (hollow circles) and 100 °C (hollow triangles).

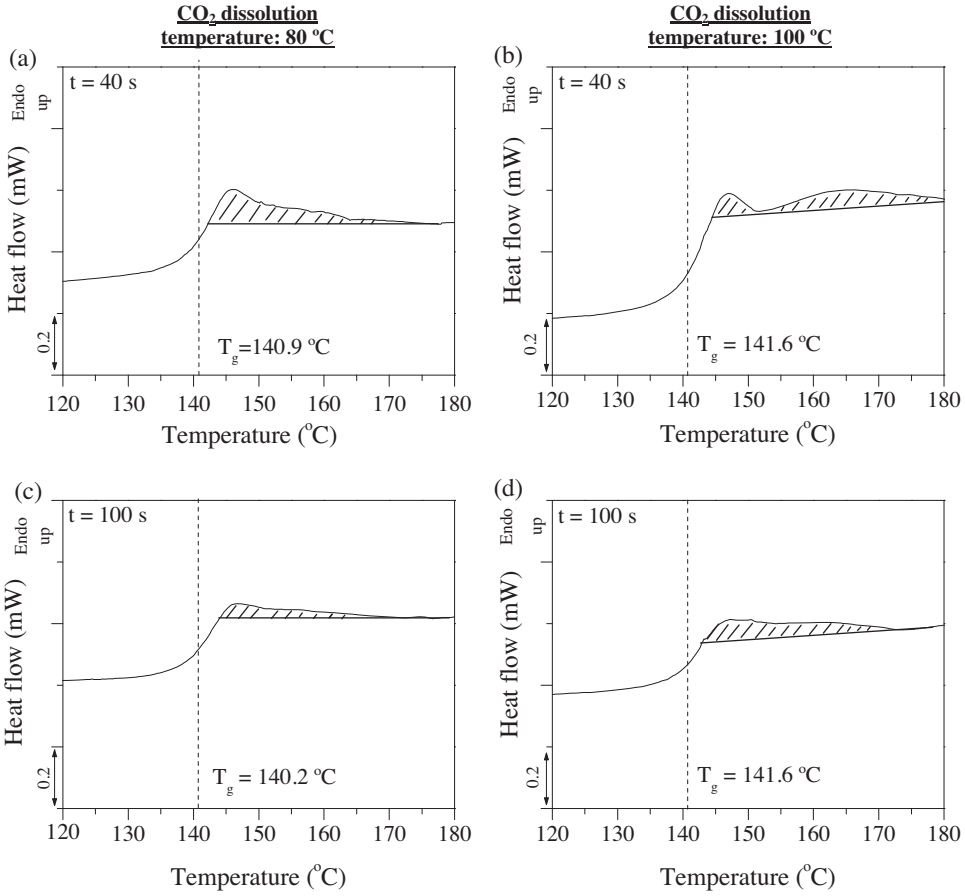


**Fig. 7.** DSC thermograms of PC foams obtained by heating during 40 s foam precursors with $CO_2$ dissolved at (a) 80 °C and (b) 100 °C and of PC foams obtained by heating during 100 s foam precursors with $CO_2$ dissolved at (c) 80 °C and (d) 100 °C.

$T_g$ of the polymer–$CO_2$ mixture, whose value was found to decrease linearly with the amount of dissolved $CO_2$, bimodal foams having both small and large cells were produced by two-step batch depressurization. PC foams having a bimodal cellular structure showed improved tensile properties when compared to the unimodal PC foams, demonstrating the direct influence of cellular structure in the mechanical performance of the resulting foams and hence the importance in controlling it.

### 3.4. *Effects of two-step foaming on the physical aging of PC*

The influence of the temperature of $CO_2$ dissolution during Stage I as well as the heating foaming time applied during Stage II on the physical aging of PC was analyzed by means of DSC. Fig. 7 presents a comparative between characteristic DSC thermograms of PC foams obtained by dissolving $CO_2$ at 80 and 100 °C in Stage I and foaming the resulting foam precursors containing $CO_2$ by applying 40 and 100 s of heating time during Stage II. First of all, PC presented physical aging in all of the prepared foams, as assessed by the relaxation observed in the glass transition (see areas indicated with crossed lines in Fig. 7). Comparatively, PC foams obtained by dissolving $CO_2$ at 100 °C presented higher values of this area, as can be seen by the higher values of the relaxation enthalpies shown in Table 3, as expected based on the fact that the higher the temperature used during $CO_2$ dissolution the higher the molecular mobility of PC induced by the well known plasticizing effect of $CO_2$ on PC [21]. This enhanced molecular mobility promoted the re-arrangement of PC molecules into a lower free-energy structure that was kinetically favourable in the presence of $CO_2$. However, in the absence of $CO_2$ after foaming, the structure went into a non-stable form. These molecules in a non-equilibrium state could not fully relax during cooling before vitrification, leading to a certain degree of molecular constraining. Although $CO_2$ dissolution promoted the molecular mobility of PC at these specific experimental conditions, there was not any sign of crystallization detected by DSC in any of the foamed samples.

The highest value of the relaxation enthalpy associated to the glass transition of PC was found for PC100-1, i.e., for the foam prepared by dissolving $CO_2$ at 100 °C in Stage I and heating during 40 s in Stage II (see Fig. 7(b) and Table 3). This is indicative of the higher amount of constrains that remained after a short heating time applied during Stage II of foaming, suggesting that the higher quantity of $CO_2$ dissolved at 100 °C (7 wt%) promoted a higher molecular mobility of PC, accelerating its physical aging.

The influence of the heating time applied during Stage II of foaming on the relaxation enthalpy associated to the glass transition of PC can be clearly observed by the characteristic thermograms presented in Fig. 7 and the values shown in Table 3. There is a clear reduction of the relaxation enthalpy for both the PC foams obtained by dissolving $CO_2$ at 80 and 100 °C with increasing the heating time applied during Stage II, which was related to an increasingly higher relaxation of PC molecules, ultimately leading to relaxation enthalpy values for the longer heating times close to that of PC in equilibrium.

**Table 3**
Glass transition temperatures and relaxation enthalpies of PC foams prepared by dissolving $CO_2$ at 80 and 100 °C.

| Heating time (s) | $CO_2$ dissolved at 80 °C | | $CO_2$ dissolved at 100 °C | |
|---|---|---|---|---|
| | $T_g$ (°C) | Relaxation enthalpy (J/g) | $T_g$ (°C) | Relaxation enthalpy (J/g) |
| 40 | 140.9 | 1.7 ± 0.2 | 141.6 | 3.3 ± 0.4 |
| 60 | 141.4 | 1.5 ± 0.2 | 141.5 | 1.8 ± 0.2 |
| 80 | 141.2 | 1.3 ± 0.2 | 141.0 | 1.6 ± 0.2 |
| 100 | 140.2 | 0.7 ± 0.1 | 141.1 | 1.4 ± 0.2 |
| 120 | 141.1 | 0.6 ± 0.1 | 141.7 | 1.2 ± 0.2 |

Although no simple correlations have been found between changes in the mechanical properties and the shift of the endothermic peak associated to the glass transition of PC resulting from physical aging [11], as changes in the mechanical properties seem to be mainly affected by volumetric changes occurring in the polymer while enthalpy relaxation depends on variations in its internal energy [12], it has been demonstrated that physical aging plays a major role in the embrittlement of PC, making it more vulnerable to stress concentrations such as microcavities [22,23], and thus is of extreme importance in terms of understanding the mechanical properties of the resulting foams.

## 4. Conclusions

It was possible to prepare closed-cell polycarbonate foams with expansion ratios taking as a reference the density of the initial solid base material of up to 14 with very different cellular morphologies using a two-step foaming process that consisted of the initial dissolution of $scCO_2$ into PC foaming precursors (Stage I) and their later expansion by heating using a double contact restriction method (Stage II).

A higher concentration of $CO_2$ was dissolved in PC with increasing the dissolution temperature in Stage I from 80 (5 wt% $CO_2$) to 100 °C (7 wt% $CO_2$), which was related to the higher molecular mobility of PC at higher temperature. Similar $CO_2$ desorption trends and diffusion coefficients were found for both dissolution conditions.

Depending on the $CO_2$ dissolution temperature used in Stage I of foaming it was possible to obtain PC foams with cellular structures that varied from isotropic-like microcellular (dissolution temperature: 80 °C) to cellular structures characterized by much bigger cells that were highly elongated in the vertical foam growth direction (dissolution temperature: 100 °C). While there was a direct correlation of the evolution of both the relative density as well as the cellular structure parameters of the foams with the heating time applied in Stage II for a $CO_2$ dissolution temperature of 100 °C, in the case of those prepared by dissolving $CO_2$ at 80 °C it was possible to increasingly reduce their relative density while keeping their microcellular structure.

Comparatively, PC foams obtained by dissolving $CO_2$ at 100 °C presented higher values of the relaxation enthalpies associated to the glass transition (physical aging) when compared to the ones obtained by dissolving $CO_2$ at 80 °C, which was related to a higher PC molecular mobility in the presence of a higher amount of $CO_2$ and non-full molecular relaxation during cooling before vitrification. There was a clear reduction of the relaxation enthalpy for both the PC foams obtained by dissolving $CO_2$ at 80 and 100 °C with increasing the heating time applied during Stage II, which could result beneficial in reducing or nearly eliminating PC's physical aging inherent to the $CO_2$ dissolution stage.

## Acknowledgement

The authors would like to acknowledge the Spanish Ministry of Economy and Competitiveness for the financial support of project MAT2011-26410.

## References

[1] Q. Lan, J. Yu, J. Zhang, J. He, Enhanced crystallization of bisphenol A polycarbonate in thin and ultrathin films by supercritical carbon dioxide, Macromolecules 44 (2011) 5743–5749.
[2] L. Chen, D. Rende, L.S. Schadler, R. Ozisik, Polymer nanocomposite foams, Journal of Materials Chemistry A 1 (2013) 3837–3850.
[3] L. Chen, L.S. Schadler, R. Ozisik, An experimental and theoretical investigation of the compressive properties of multi-walled carbon nanotube/poly(methyl methacrylate) nanocomposite foams, Polymer 52 (2011) 2899–2909.
[4] J.A.R. Ruiz, J. Marc-Tallon, M. Pedros, M. Dumon, Two-step micro cellular foaming of amorphous polymers in supercritical $CO_2$, Journal of Supercritical Fluids 57 (2011) 87–94.
[5] M.-T. Liang, C.-M. Wang, Production of engineering plastics foams by supercritical $CO_2$, Industrial and Engineering Chemistry Research 39 (2000) 4622–4626.
[6] G. Gedler, M. Antunes, V. Realinho, J.I. Velasco, Thermal stability of polycarbonate–graphene nanocomposite foams, Polymer Degradation and Stability 97 (2012) 1297–1304.
[7] V. Kumar, J. Weller, Production of microcellular polycarbonate using carbon dioxide for bubble nucleation, Journal of Engineering for Industry 116 (1994) 413–420.
[8] Y. Ito, M. Yamashita, M. Okamoto, Foam processing and cellular structure of polycarbonate-based nanocomposites, Macromolecular Materials and Engineering 291 (2006) 773–783.
[9] J.E. Weller, V. Kumar, Solid-state microcellular polycarbonate foams. I. The steady-state process space using subcritical carbon dioxide, Polymer Engineering and Science 50 (2010) 2160–2169.
[10] L.C.E. Struik, Physical Aging in Amorphous Polymers and Other Materials, Elsevier, Amsterdam, 1978.
[11] J.M. Hutchinson, S. Smith, B. Horne, G.M. Gourlay, Physical aging of polycarbonate: enthalpy relaxation, creep response, and yielding behavior, Macromolecules 32 (1999) 5046–5061.
[12] V.A. Soloukhin, J.C.M. Brokken-Zijp, O.L.J. van Asselen, G. de With, Physical aging of polycarbonate: elastic modulus, hardness, creep, endothermic peak, molecular weight distribution, and infrared data, Macromolecules 36 (2003) 7585–7597.
[13] H. Soma, S. Nishitsuji, T. Inoue, Molecular weight dependence in a relaxation phenomenon at glassy state: physical aging of polycarbonate, Polymer 53 (2012) 895–896.
[14] Z.Z. Nawaby, Solubility and diffusivity in thermoplastic foam processing, in: S.T. Lee (Ed.), Thermoplastic Foam Processing: Principles and Development, CRC Press, London, 2005.
[15] Y.W. Cheung, R.S. Stein, Critical analysis of the phase behavior of poly(epsilon-caprolactone) (PCL)/polycarbonate (PC) blends, Macromolecules 27 (1994) 2512–2519.
[16] G. Sims, C. Khunniteekool, Cell size measurement of polymeric foams, Cellular Polymers 13 (1994) 137–146.
[17] C.H. Ho, T. Vu-Khanh, Effects of time and temperature on physical aging of polycarbonate, Theoretical and Applied Fracture Mechanics 39 (2003) 107–116.
[18] M. Tang, T.-B. Du, Y.-P. Chen, Sorption and diffusion of supercritical carbon dioxide in polycarbonate, Journal of Supercritical Fluids 28 (2004) 207–218.
[19] M. Tang, W.-H. Huang, Y.-P. Chen, Comparisons of the sorption and diffusion of supercritical carbon dioxide into polycarbonate and polysulfone, Journal of the Chinese Institute of Chemical Engineers 38 (2007) 419–424.
[20] Z. Ma, G. Zhang, Q. Yang, X. Shi, A. Shi, Fabrication of microcellular polycarbonate foams with unimodal or bimodal cell-size distributions using supercritical

carbon dioxide as a blowing agent, Journal of Cellular Plastics 50 (2014) 55–79.
[21] X. Liao, J. Wang, G. Li, J. He, Effect of supercritical carbon dioxide on the crystallization and melting behavior of linear bisphenol A polycarbonate, Journal of Polymer Science Part B: Polymer Physics 42 (2004) 280–285.
[22] D.J.A. Senden, T.A.P. Engels, S.H.M. Sontjens, L.E. Govaert, The effect of physical aging on the embrittlement of steam-sterilized polycarbonate, Journal of Materials Science 47 (2012) 6043–6046.
[23] D.J.A. Senden, J.A.W. van Dommelen, L.E. Govaert, Physical aging and deformation kinetics of polycarbonate, Journal of Polymer Science Part B: Polymer Physics 50 (2012) 1589–1596.